REGULAR ARTICLE

blood advances

Uptake of long-chain fatty acids from the bone marrow suppresses CD8$^+$ T-cell metabolism and function in multiple myeloma

Nancy Gudgeon,[1] Hannah Giles,[2] Emma L. Bishop,[1] Taylor Fulton-Ward,[1] Cristina Escribano-Gonzalez,[3] Haydn Munford,[1] Anna James-Bott,[4] Kane Foster,[5] Farheen Karim,[6] Dedunu Jayawardana,[6] Ansar Mahmood,[2] Adam P. Cribbs,[4] Daniel A. Tennant,[3] Supratik Basu,[6] Guy Pratt,[1,2] and Sarah Dimeloe[1,3]

[1]Institute of Immunology and Immunotherapy, College of Medical and Dental Sciences, University of Birmingham, Birmingham, United Kingdom; [2]Centre for Clinical Haematology, University Hospitals Birmingham NHS Trust, Birmingham, United Kingdom; [3]Institute of Metabolism and Systems Research, College of Medical and Dental Sciences, University of Birmingham, Birmingham, United Kingdom; [4]Nuffield Department of Orthopaedics, Botnar Research Centre, Rheumatology and Musculoskeletal Sciences, National Institute of Health Research Oxford Biomedical Research Unit, University of Oxford, Oxford, United Kingdom; [5]Research Department of Haematology, UCL Cancer Institute, University College London, London, United Kingdom; and [6]Clinical Haematology Unit, Royal Wolverhampton Hospitals NHS Trust, Wolverhampton, United Kingdom

Key Points

- CD8$^+$ T-cell function and mitochondrial mass decline in the bone marrow in MM and are lower than in matched peripheral blood.
- These changes are linked to uptake of long-chain fatty acids, and T-cell function can be rescued by blockade of the lipid transporter FATP1.

T cells demonstrate impaired function in multiple myeloma (MM) but suppressive mechanisms in the bone marrow microenvironment remain poorly defined. We observe that bone marrow CD8$^+$ T-cell function is decreased in MM compared with controls, and is also consistently lower within bone marrow samples than in matched peripheral blood samples. These changes are accompanied by decreased mitochondrial mass and markedly elevated long-chain fatty acid uptake. In vitro modeling confirmed that uptake of bone marrow lipids suppresses CD8$^+$ T function, which is impaired in autologous bone marrow plasma but rescued by lipid removal. Analysis of single-cell RNA-sequencing data identified expression of fatty acid transport protein 1 (FATP1) in bone marrow CD8$^+$ T cells in MM, and FATP1 blockade also rescued CD8$^+$ T-cell function, thereby identifying this as a novel target to augment T-cell activity in MM. Finally, analysis of samples from cohorts of patients who had received treatment identified that CD8$^+$ T-cell metabolic dysfunction resolves in patients with MM who are responsive to treatment but not in patients with relapsed MM, and is associated with substantial T-cell functional restoration.

Introduction

Despite observations of T-cell dysfunction in multiple myeloma (MM),[1-9] checkpoint blockade therapies have not been successful,[10,11] indicating that alternative suppressive mechanisms operate in the MM bone marrow (BM) microenvironment. The identification of such mechanisms will therefore inform novel approaches to augment antitumor function of endogenous and therapeutic T cells in MM.

Upon antigen recognition, T cells alter their metabolism to support clonal expansion and effector functions.[12,13] They take up more glucose and amino acids and alter metabolic pathway usage to support their anabolic effector program. Increased conversion of pyruvate to lactate enables rapid glycolytic flux, generating biosynthetic precursors. Mitochondrial biogenesis and elevated glucose and

Submitted 31 January 2023; accepted 19 May 2023; prepublished online on *Blood Advances* First Edition 5 June 2023; final version published online 11 October 2023. https://doi.org/10.1182/bloodadvances.2023009890.

RNA-sequencing data were accessed from GEO GSE186448 and GSE139369.

Data are available on request from the corresponding author, Sarah Dimeloe (s.k.dimeloe@bham.ac.uk).

The full-text version of this article contains a data supplement.

glutamine oxidation support signaling, transcription, and translation through generation of reactive oxygen species, tricarboxylic acid cycle intermediates and adenosine triphosphate.

This dependence on augmented metabolism renders T cells susceptible to their microenvironment. Within solid tumors, nutrient competition limits T-cell function,[14-16] whereas chronic antigen exposure under hypoxia drives mitochondrial dysfunction.[17,18] Recently, immune cell lipid uptake from tumor microenvironments has been linked to loss of function. For example, in models of pancreatic ductal adenocarcinoma, melanoma, and obesity-promoted breast cancer, infiltrating $CD8^+$ T and natural killer (NK) cells accumulate long-chain fatty acids, which impair mitochondrial fitness and immune function, and can induce lipid peroxidation–driven cell death by ferroptosis.[19-25] Notably, blocking lipid uptake, targeting associated transcription factors, or restoring normal lipid metabolism improves immune cell function in these microenvironments.

The capacity of microenvironmental lipids to suppress T cells in MM has not been assessed but may be pertinent, given that the BM is a lipid-rich environment, particularly in disease. Adipocytes are a major BM component, comprising up to 70% of its volume in older adults[26]; obesity increases this, and both age and obesity are independent risk factors for MM progression.[27] In turn, once MM develops, MM plasma cells (MMPCs) further promote adipogenesis[28] and induce BM adipocyte lipolysis, taking up released lipids to support their growth and survival.[29] Consequently, T cells also encounter an enriched lipid environment in the MM BM but the impact on their function is unknown.

In this study, we assessed T-cell phenotype, function, and metabolic capacity in matched peripheral blood (PB) and BM samples across the spectrum of MM, including at premalignant stages of disease and after treatment, to interrogate whether T-cell metabolism is altered with MM progression, and, importantly, how this relates to their function in the MM BM microenvironment and whether it can be targeted to augment T-cell activity.

Materials and methods

Patient cohort, sample collection, and cell isolation

BM aspirates and PB samples were obtained from patients with monoclonal gammopathy of undetermined significance (MGUS), asymptomatic MM, and MM at diagnosis, on relapse, and in remission, recruited from hematology clinics at University Hospitals Birmingham and The Royal Wolverhampton Hospitals National Health Service Trusts (supplemental Tables 1 and 2). Age-matched controls were recruited from University Hospitals Birmingham National Health Service Trust via the Human Biomaterials Resource Centre. Control BM samples were taken from the femoral head during planned orthopedic surgery (6/10) or after trauma (4/10). The study received ethical approval (references: 10/H1206/58 and 20/NW/0001) and informed written consent was obtained. Mononuclear cells were isolated by density-gradient centrifugation using Ficoll-Paque (Cytiva, catalog #17144003), harvested, washed with phosphate-buffered saline (Sigma, catalog #D8537), counted, and frozen in freezing medium (10% dimethyl sulfoxide, Sigma, catalog #472301 and 90% fetal calf serum [FCS], Sigma, catalog #F9665). Plasma was frozen at −80°C.

Analysis of mononuclear cells by flow cytometry

Mononuclear cells were thawed, washed twice in RPMI 1640 medium (Sigma, catalog #R8758), resuspended at 1×10^6 cells per mL in RPMI 1640 medium containing 10% FCS and penicillin (100 U/mL)/streptomycin (0.1 mg/mL) (in RPMI/FCS; Sigma, catalog #P4333), and interleukin 2 (IL-2; 50 IU/mL; Peprotech, catalog #200-02), and then rested at 37°C under 5% CO_2 for 16 hours. Cells were stained for viability with efluor780 (Invitrogen, catalog #13539140) and fluorophore-conjugated antibodies for cell-surface markers (supplemental Table 3), together with 50 nM Mitoview Green (MVG; Cambridge Bioscience, catalog #70054), 1 μM Bodipy-C_{16} (Invitrogen catalog #D3821), or 2.5 μM Bodipy 581/591 (Thermofisher, Cat #D3861) in RPMI/FCS for 20 minutes at 37°C under 5% CO_2. Cells were washed twice with phosphate-buffered saline/1% FCS and analyzed using a BD LSRFortessa X-20 flow cytometer. For intracellular cytokine staining, T cells were stimulated using Immunocult CD3/CD28 T-cell activator (StemCell, catalog #109910) and Brefeldin A (10 μg/mL; Acros organics, catalog #297140050) for 4 hours, stained for viability and cell-surface markers before fixation/permeabilization (FoxP3 buffer set, eBioscience Inc, catalog #00-5523-00) and staining with anticytokine fluorophore-conjugated antibodies (supplemental Table 3). For CoxIV staining, cells were stimulated with T-cell activator, fixed and permeabilized, stained with anti-CoxIV-AF647 (Abcam catalog #ab197491), and blocked with mouse serum before staining for surface markers and cytokines, as described. Mitochondrial mass and lipid-uptake capacity were analyzed as mean fluorescence intensity (MFI) for MVG and Bodipy-C_{16}, which were normalized to the average for each batch of samples analyzed concurrently. Lipid peroxidation capacity was calculated as the ratio of Bodipy 581/591 MFI at 510 nm (emission after lipid peroxidation) to Bodipy 581/591 MFI at 590 nm (emission before lipid peroxidation) in the same sample.

Autologous plasma experiments

BM mononuclear cells were thawed, washed twice in RPMI 1640 medium, and resuspended at 1×10^6 cells per mL in 50% RPMI 1640/FCS and 50% autologous PB or BM plasma. Where indicated, BM plasma was stripped of lipids using CleanAscite (Caltag, catalog #X2555-10), or additions were made: SSO (CD36 agonist, 100 μM; Cambridge Biosciences catalog #11211), ferrostatin (inhibitor of lipid peroxidation, 1 μM; Selleckchem, catalog #S7243), fatty acid transport protein 1 (FATP1)-IN-2 (an FATP1 inhibitor, 1 μM; Medchem express, catalog #HY-141700), or ursodeoxycholic acid (an FATP5 inhibitor, 10 μM; Sigma, catalog #PHR1579). T cells were stimulated for 48 hours and analyzed for cell-surface marker expression, mitochondrial mass, and cytokine expression by flow cytometry. Cells stained for cytokines were first stimulated for 4 hours with a cell-activation cocktail (BioLegend, catalog #423304). Cell culture supernatants from 0.2×10^6 cells were harvested and stored at −20°C for analysis of cytokine concentration by enzyme-linked immunosorbent assay (ELISA).

ELISA

Interferon gamma (IFN-γ) in supernatants was measured by ELISA using anti–IFN-γ capture (Bio-Rad, Clone AbD00676, catalog #HCA043) and biotinylated detection (Bio-Rad, Clone 2503 catalog #HCA044P) antibodies, recombinant IFN-γ standard (Bio-Rad, catalog #PHP050), streptavidin-HRP (Sigma Aldrich,

catalog #E2866), and 3,3′,5,5′-tetramethylbenzidine substrate (Bio-Rad, catalog #BUF062B). Tumor necrosis factor α (TNF-α) in supernatants was measured by ELISA, using an TNF ELISA kit (Invitrogen, CHC1753 and CNB0011) per the manufacturer's instructions.

Plasma-cell abundance

Plasma-cell abundance was assessed in diagnostic first-pull BM aspirate samples. Sample smears were assessed morphologically on slides with May-Grümwald-Giemsa staining.

Data analysis

Flow cytometry data were analyzed using FlowJo version 10 (TreeStar Ltd). Statistical analysis was undertaken using GraphPad Prism version 9.3. Statistical tests used are indicated in the figure legends.

Results

BM CD8$^+$ T-cell function declines in MM and is consistently lower than in matched PB

Phenotyping of major T-cell subsets in BM and PB mononuclear cells from age-matched controls, individuals with MGUS, asymptomatic MM, and MM at diagnosis identified that BM CD8$^+$ T-cell abundance decreased with disease development and was significantly reduced in MM at diagnosis compared with controls (supplemental Figure 1A; Figure 1A). In contrast, frequencies of BM CD4$^+$ T cells (Figure 1B) as well as PB CD8$^+$ and CD4$^+$ T cells remained similar (supplemental Figure 1B-C). BM CD56$^+$ NK cell abundance also did not change with disease development, whereas CD4$^+$CD127$^-$CD25$^+$ regulatory T cells (TRegs) were enriched in MM BM at diagnosis compared with in control BM, which is in agreement with literature (supplemental Figure 1A,D-E).[5,7] In PB samples, NK cell and TReg frequencies were similar at all disease stages (supplemental Figure 1D-E). Next, we assessed the proportion of T cells within BM and PM samples expressing the key antitumor cytokines IFN-γ and TNF-α as well as IL-2 and the cytotoxic molecule granzyme B. We noted interindividual variability for a number of these readouts, which should be taken into account, but identified decreased frequencies of IFN-γ– and IL-2–expressing CD8$^+$ T cells, as well as multifunctional CD8$^+$ T cells expressing all 3 cytokines, and those expressing granzyme B in MM BM compared with controls (Figure 1C). Frequencies of CD4$^+$ T cells expressing these molecules did not change significantly (Figure 1D). These observations were specific to BM CD8$^+$ T cells, whereas PB T-cell cytokine and granzyme expression also did not change (supplemental Figure 1F-G) Indeed, pairwise comparison of BM and PB samples identified that CD8$^+$ T cells were consistently less functional within BM samples than in matched PB samples. Frequencies of IFN-γ–, TNF-α–, IL-2–, and granzyme B–expressing CD8$^+$ T cells appeared lower in the BM than in the PB in all patient groups, including controls, albeit the disparity increased with disease development for IFN-γ and TNF-α. When all patient samples were combined, this difference was highly significant (Figure 1E; supplemental Figure 1H). However, this was not the case for CD4$^+$ T cells, which demonstrated similar functionality within BM and PB samples, and for increased multifunctional cells in the BM in controls (Figure 1F; supplemental Figure 1I), indicating that CD8$^+$ T-cell function specifically is decreased within the BM microenvironment compared with the within periphery. Expression of cytokines was largely restricted to memory populations of T cells, as shown in example flow plots from 1 sample from a patient with asymptomatic MM, with CD45RA$^+$CCR7$^-$ terminally differentiated effector memory (EM) CD8$^+$ T cells being a significant source of IFN-γ, TNF-α, and granzyme B but not IL-2 (Figure 1G), and CD45RA$^-$CCR7$^-$ EM CD4$^+$ T cells being the major IFN-γ expressers, with contribution of CD45RA$^-$CCR7$^+$ central memory (CM) cells for TNF-α (Figure 1H). However, proportions of these subpopulations were broadly similar between the BM and PB at all disease stages (Figure 1I-J), meaning that the altered overall function of CD8$^+$ T cells in the BM vs the PB is not explained by enrichment or loss of functionally distinct subpopulations, and could rather relate to an effect of the microenvironment.

CD8$^+$ T-cell mitochondrial mass and lipid uptake are altered during progression of MM and in the BM microenvironment

T-cell function is underpinned by metabolic capacity, particularly mitochondrial mass.[12,13] Analysis of BM T-cell mitochondrial mass using the fluorescent probe MVG revealed that it was reduced within CD8$^+$ and CD4$^+$ T cells in MGUS, asymptomatic MM, and MM at diagnosis compared with controls (Figure 2A-B). Similar to immune effector function however, these changes were less apparent in matched PB samples (supplemental Figure 2A-B). Of note, BM CD8$^+$ T cells again demonstrated significantly reduced mitochondrial mass compared with paired PB cells when all patient samples were grouped (Figure 2C), which was not the case for CD4$^+$ T cells (Figure 2D), indicating a potential link between decreased mitochondrial mass and reduced functionality of CD8$^+$ T cells in the BM microenvironment. To directly interrogate the relationship between mitochondrial mass and immune effector function, we stained for CoxIV, a subunit of ETC complex IV, as a mitochondrial marker, together with cytokines (because MVG cannot be fixed for intracellular staining) in a subset of samples from controls and patients with MM at diagnosis. There was a clear trend for CoxIV expression to be higher in cytokine-expressing CD8$^+$ T and CD4$^+$ T cells than in cytokine-negative populations (Figure 2E; supplemental Figure 2D), supporting a relationship between mitochondrial mass and effector function. In these assays, TNF-α expression was more tightly linked to CoxIV abundance than IFN-γ expression, potentially explained by the well-documented relationship between glycolysis and IFN-γ expression in CD8$^+$ T cells.[30,31] Further confirmation that mitochondrial mass is related to T-cell effector function across this patient cohort was provided by correlative analyses of MVG fluorescence vs frequency of cytokine-expressing cells in the BM sample, which identified significant positive relationships for IFN-γ– and TNF-α–expressing CD8$^+$ T cells, as well as IFN-γ– TNF-α–, IL-2–expressing T-cell subsets and multifunctional CD4$^+$ T-cell subsets (Figure 2F; supplemental Figure 2D).

Long-chain fatty acid uptake from tumor microenvironments is increasingly implicated in immune cell suppression through mechanisms including mitochondrial loss and dysfunction[19,20] and lipid peroxidation–induced ferroptosis.[23,32] This may be pertinent in the lipid-rich BM, in which decreased mitochondrial mass of CD8$^+$ T cells was observed; therefore, capacity of T cells to take up long-chain fatty acids was assessed using a fluorescent palmitate probe,

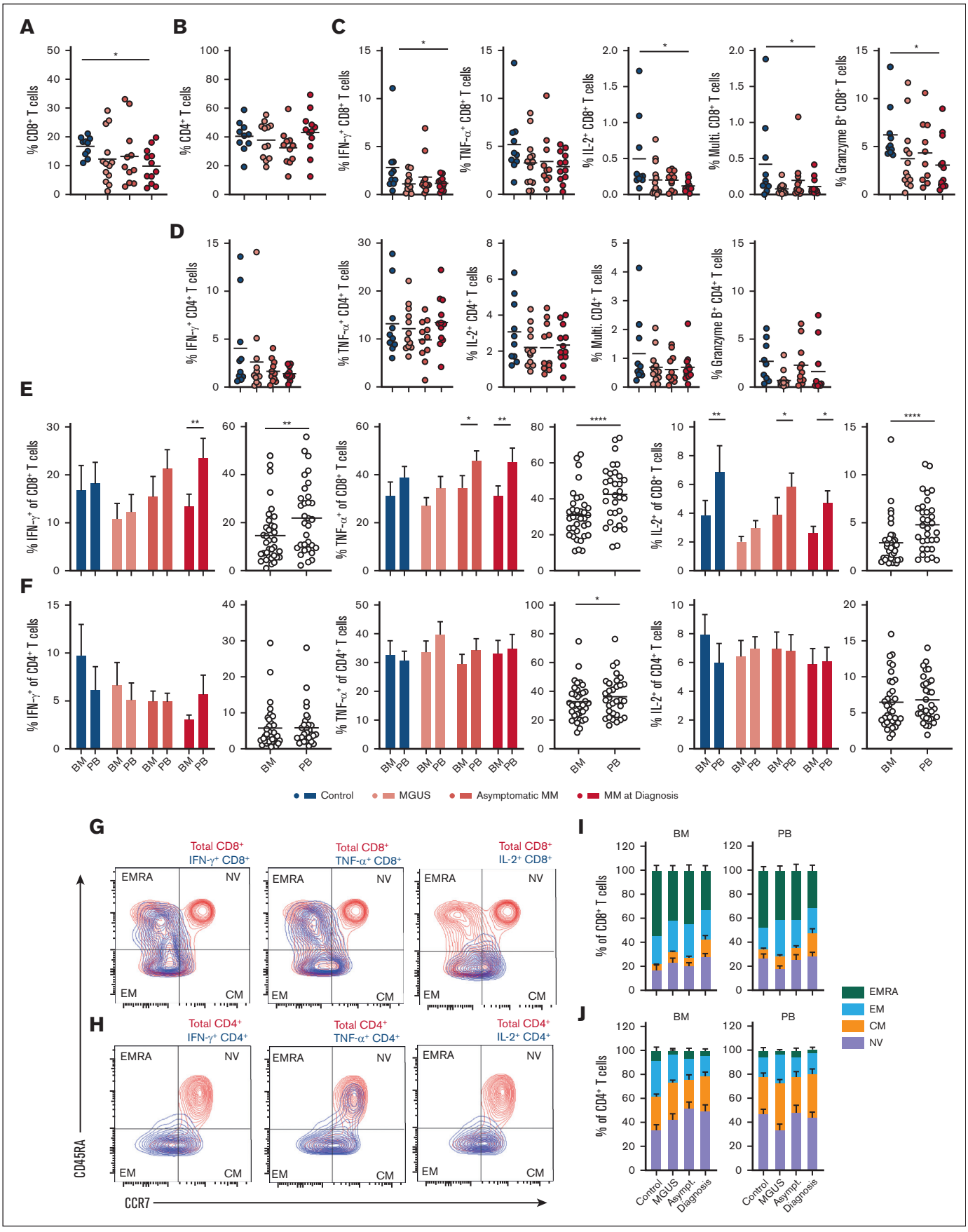

Figure 1.

C_{16}-BODIPY. Uptake of this probe was similar in BM and PB T cells across all disease stages (Figure 2G; supplemental Figure 2E-F) but markedly elevated in BM cells, particularly $CD8^+$ T cells compared with PB populations (Figure 2H-I; supplemental Figure 2G). Among $CD8^+$ T cells, C_{16}-BODIPY uptake mapped, in particular, to antigen-experienced CM and EM populations and was also significantly higher in cells expressing the immune checkpoints TIGIT and PD-1 than in checkpoint-negative cells (Figure 2J). Lipid peroxidation within T cells from patients with MM was also assessed using BODIPY 581/591, which fluoresces at different wavelengths before and after peroxidation. This identified that, in addition to increased lipid-uptake capacity, BM T cells also demonstrate elevated lipid peroxidation compared with PB T cells (Figure 2K; supplemental Figure 2H). This is consistent with findings in other tumor microenvironments and may relate to changes in mitochondrial content and effector function.[32]

$CD8^+$ T-cell function is impaired by lipid uptake from the BM microenvironment via FATP1

Next, we established an in vitro model to interrogate the relationship between long-chain fatty acid uptake and T-cell mitochondrial and immune dysfunction within the BM microenvironment. Specifically, we cultured BM mononuclear cells from control individuals or patients with MM in autologous PB or BM plasma, stimulated T cells, and assessed their mitochondrial mass and cytokine production. This established that BM plasma significantly decreased mitochondrial mass and IFN-γ expression by $CD8^+$ T cells compared with PB plasma, and this occurred in both control and MM samples (Figure 3A-B). In contrast, $CD4^+$ T-cell mitochondrial mass was not altered in BM plasma, despite reduced IFN-γ expression (supplemental Figure 3A-B). Total secreted IFN-γ was also decreased in BM plasma cultures, as was TNF-α (Figure 3C-D). Next, to probe a role for lipids in this suppressive activity of BM plasma, lipids were depleted from BM samples and compared with lipid-replete BM samples. Removal of BM lipids increased mitochondrial mass in control and MM BM $CD8^+$ T cells (Figure 3E), accompanied by restoration of IFN-γ and TNF-α expression (Figure 3F-H). In $CD4^+$ T cells, however, mitochondrial mass remained unchanged, whereas IFN-γ expression was not restored (supplemental Figure 3C-D), indicating an alternative, lipid-independent mechanism of suppression, in line with patient data. Taken together, the data indicate that BM $CD8^+$ T cells substantially take up lipids from the BM environment, leading to loss of mitochondrial mass and impaired functionality. This occurs in control BM, consistent with decreased functionality of BM vs PB $CD8^+$ T cells (Figure 1), but may compound disease-driven loss of T-cell mitochondrial mass (Figure 2) to further compromise BM $CD8^+$ T-cell function in MM. To probe a role for lipid peroxidation–induced damage in $CD8^+$ T cell dysfunction, BM mononuclear cell cultures were treated with ferrostatin, a synthetic antioxidant that inhibits lipid peroxidation. This increased IFN-γ secretion in BM plasma but not in PB plasma (Figure 3I-K), confirming that BM lipid peroxidation contributes to T-cell suppression.

Because BM lipids suppress $CD8^+$ T-cell function, it is possible that effective blockade of relevant transporters may therefore restore this within the BM environment. With this aim, we set out to identify candidate lipid transporters. The long-chain fatty acid transporter CD36 is implicated in mediating immune-suppressive and ferroptotic effects of lipids on NK and T-cell populations.[19,23] We therefore assessed its expression in BM samples and found it to be more highly expressed by $CD8^+$ than $CD4^+$ T cells (Figure 3L; supplemental Figure 3E), consistent with C_{16}-BODIPY uptake data. However, analysis of cytokine expression revealed that $CD36^+$ cells more highly expressed IFN-γ, TNF-α, and IL-2 than $CD36^-$ counterparts, indicating that activity of this transporter may not suppress BM T-cell function (Figure 3M; supplemental Figure 3F). Consistent with this, CD36 blockade with the irreversible agonist SSO did not increase $CD8^+$ or $CD4^+$ T-cell IFN-γ expression in BM plasma (Figure 3N; supplemental Figure 3G) and indeed decreased overall IFN-γ secreted (Figure 3O). Therefore, to identify other relevant transporters expressed by BM $CD8^+$ T cells, we explored single-cell RNA-sequencing analysis of BM mononuclear cells isolated from 2 patients with newly diagnosed MM.[33] Specifically, within these data we assessed expression of the FATPs 1 to 6 (FATP1 through FATP6; SLC27A1-6). These proteins mediate uptake of long-chain fatty acids and convert them into acyl-CoA esters, which are retained within the cell. This analysis identified that FATP1 and FATP5 are the most highly expressed family members in BM $CD8^+$ T cells in MM, whereas transcripts for FATP2, FATP4 and FATP6 were scarce and were undetectable for FATP3 (Figure 3P). Analysis of a BM single-cell RNA-sequencing data set with cellular indexing of transcriptomes and epitopes by sequencing data[34] from 2 healthy donor samples revealed broadly similar expression patterns, with FATP1 and FATP5 being more highly expressed than FATP2, FATP4, or FATP6 (undetectable in this data set) (supplemental Figure 3H-I). In contrast, FATP3 was more abundant in control BM than in MM BM, yet the significance of this is unclear because FATP3 does not have confirmed lipid-uptake activity nor localize to the plasma membrane, indeed very little is known about the function of this family member.[35] We therefore assessed whether blockade of FATP1 with FATP1in2, or FATP5 with ursodeoxycholic acid, could restore function of $CD8^+$ T cells from patients with MM activated in presence of autologous BM or PB plasma. These experiments identified that blockade of FATP1 or FATP5 in PB plasma–treated $CD8^+$ T cells had no effect on IFN-γ production (Figure 3Q;

Figure 1. BM $CD8^+$ T-cell function declines in MM and is consistently lower than in matched PB. (A-B) Proportion of (A) $CD8^+$ and (B) $CD4^+$ T cells within BM FSC/SSC-low cells from controls (n = 10), individuals with MGUS (n = 13), asymptomatic MM (asymptomatic; n = 11), or MM at diagnosis (diagnosis; n = 12). (C-D) Proportion of BM FSC/SSC-low cells from indicated groups expressing (C) CD8 or (D) CD4 and IFN-γ, TNF-α, IL-2, all 3 cytokines (multifunctional), or granzyme B, as indicated, after 4 hours stimulation via CD3/CD28 in presence of Brefeldin A. (E-F) Proportion of (E) $CD8^+$ and (F) $CD4^+$ T cells within BM or PB FSC/SSC-low cells from indicated groups expressing IFN-γ, TNF-α, or IL-2 after 4 hours stimulation as in panels C-D. Proportions within the BM and PB are directly compared for each group individually and for all patients combined. (G-H) Representative contour plots indicate memory phenotypes of BM (G) $CD8^+$ and (H) $CD4^+$ T cells expressing indicated cytokine (blue) overlaid onto total populations (red). (I-J) Proportions of naïve (NV), CM, EM, and terminally differentiated effector memory (EMRA) BM and PB $CD8^+$ and $CD4^+$ T cells are summarized at indicated disease stages. For panels A-D, significance was calculated using 1-way analysis of variance (ANOVA) or for panels E-F (bars) and I-J, 2-way ANOVA and Sidak multiple comparison tests; and for panels E-F (circles), paired *t* test between overall paired samples; $^*P < .05$, $^{**}P < .01$, $^{***}P < .0001$, and $^{****}P < .00001$.

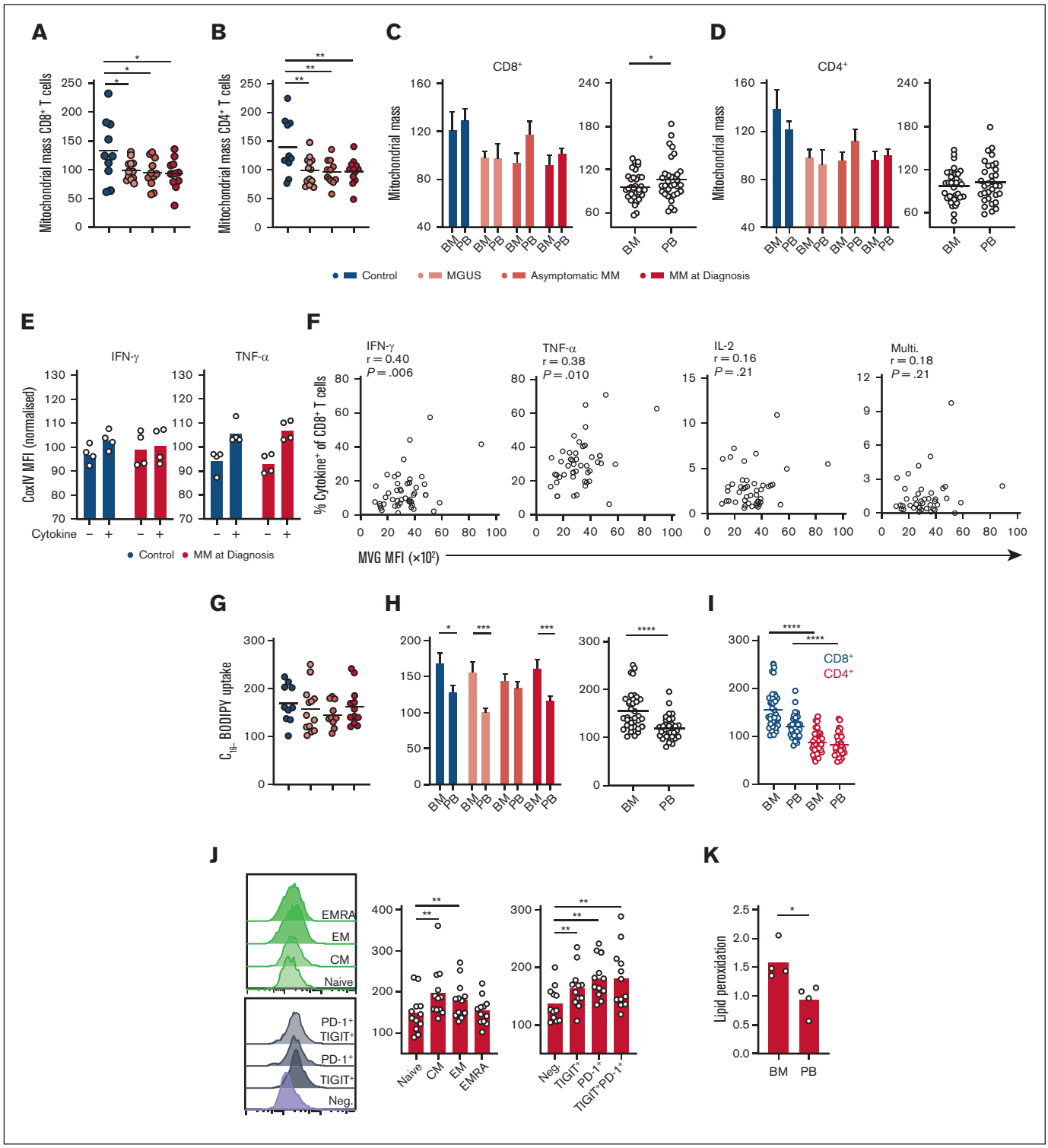

Figure 2. CD8$^+$ T-cell mitochondrial mass and long-chain fatty acid uptake are altered during progression of MM and in the BM microenvironment. (A-B) Mitochondrial mass of (A) CD8$^+$ and (B) CD4$^+$ T cells within BM mononuclear cells from controls (n = 10), individuals with MGUS (n = 13), asymptomatic MM (asymptomatic; n = 11), or MM at diagnosis (diagnosis; n = 12) was assessed by flow cytometry using MVG and is expressed relative to the mean of each experiment. (C-D) Mitochondrial mass of BM and PB CD8$^+$ and CD4$^+$ T cells is directly compared for each group and for all patient samples combined. (E) CoxIV MFI of CD8$^+$ T cells positive or negative for IFN-γ or TNF-α as indicated from control (n = 4) or MM at diagnosis (n = 4) samples. (F) Correlation of mitochondrial mass (MVG fluorescence) with frequency of BM CD8$^+$ T cells positive (+) for the indicated cytokines for all patient samples combined. (G) C_{16}-BODIPY uptake of BM CD8$^+$ T cells within indicated groups expressed relative to the mean of each experiment. (H) C_{16}-BODIPY uptake of BM and PB CD8$^+$ T cells is directly compared for each group and for all patient samples combined. (I) C_{16}-BODIPY uptake of BM

supplemental Figure 3J). However, specific blockade of FATP1, but not FATP5, significantly increased IFN-γ secretion in cells cultured in BM plasma, indicating a specific effect of BM long-chain fatty acids transported via FATP1 on $CD8^+$ T cells (Figure 3R-S; supplemental Figure 3K). Therefore, BM long-chain fatty acids decrease $CD8^+$ T-cell mitochondrial mass and impair their effector function, which can be rescued by blockade of the lipid transporter FATP1.

Functional and metabolic features of $CD8^+$ T cells are restored in patients with MM in remission but not in patients who have relapsed

Finally, to understand T-cell functional and metabolic phenotypes associated with poor vs effective control of MM, we analyzed samples from patients who had either relapsed on therapy or were in remission. In both groups, irrespective of treatment response, compared with patients with MM at diagnosis, $CD8^+$ T-cell frequency was increased in the BM and PB (Figure 4A; supplemental Figure 4A), and decreased $CD4^+$ T-cell frequency was observed in the BM and PB of patients who had received treatment compared with in those at diagnosis. (Figure 4B; supplemental Figure 4B). Proportions of naïve, CM, EM, and terminally differentiated EM $CD8^+$ and $CD4^+$ T-cell subsets were also similar between patient groups, in the BM and PB (Figure 4C-D; supplemental Figure 4C-D), as were proportions of immune-checkpoint expressing cells (Figure 4E-F; supplemental Figure 4E-F). However, clear differences between the 2 groups emerged when interrogating T-cell function and metabolism, particularly within BM $CD8^+$ T-cell populations. Proportions of these cells expressing IFN-γ, TNF-α, IL-2, and granzyme B (Figure 4G), as well as $CD4^+$ T-cells expressing IL-2 (Figure 4H), were all significantly increased in patients in remission compared with those who had relapsed. This increased functionality was less pronounced for PB $CD8^+$ T cells (supplemental Figure 4G), albeit increases in PB $CD4^+$ T-cell function were observed (supplemental Figure 4H). Frequency of multifunctional, and IFN-γ–, TNF-α–, and IL-2–expressing BM $CD8^+$ T cells inversely correlated with malignant plasma cell abundance within aspirate samples from patients with MM at diagnosis, upon relapse, and in remission (Figure 4I), supporting a role for BM $CD8^+$ T cells controlling disease progression. This was also true for TNF-α– and IL-2–expressing and multifunctional $CD4^+$ T cells (supplemental Figure 4I). Plasma cell abundance was determined from clinical diagnostic liquid morphology slides with May-Grümwald-Giemsa staining. Of note, the profound restoration in BM $CD8^+$ T-cell function in patients in remission occurred alongside significantly decreased long-chain fatty acid uptake and increased mitochondrial mass, such that, in this group, BM and PB $CD8^+$ T-cell mitochondrial mass were now comparable (Figure 4J-K). Although drivers of these metabolic and functional T-cell changes cannot easily be determined from these cross-sectional samples from patients on diverse treatment regimens (supplemental Table 2), the data nevertheless highlight that effective MM control associates with specific changes in T-cell metabolism, suggesting that strategies to modulate this, such as FATP1 blockade, could be beneficial.

Discussion

In this study, analysis of T-cell phenotype and function identified decreased abundance of total and cytokine-expressing BM $CD8^+$ T cells in patient with MM compared with in controls. This agrees with studies reporting diminished T-cell IFN-γ expression in MM[1-3,36] and indicates additional impairments in IL-2 and granzyme B. Loss of T-cell function during MM development may be partly explained by the corresponding loss of mitochondrial mass, which is well described to critically underpin T-cell function. In agreement, mitochondrial mass correlated with T-cell cytokine expression but was decreased in MM compared with in controls, and indeed in earlier disease stages. This was not observed in PB samples, indicating that it is driven by the BM microenvironment, consistent with reports that chronic stimulation under hypoxia diminishes T-cell respiratory capacity through suppression of peroxisome proliferator-activated receptor gamma coactivator 1-α (PGC1-α).[18] The BM microenvironment has low oxygen availability,[37] likely further reduced by MMPC expansion. Another important metabolic determinant of T-cell function is capacity to take up and metabolize glucose. However, assessment of T-cell glucose uptake capacity was limited by lack of reliable probes,[38] therefore it remains unclear whether this is affected by MM.

At all stages of disease and in control individuals, BM $CD8^+$ T cells demonstrated reduced functionality compared with those in matched PB. The MM BM microenvironment is described as hostile for T-cell function[39]; yet, mechanisms underpinning this remain poorly understood. Here, we observed that decreased $CD8^+$ T-cell functionality in the BM is coupled with reduced mitochondrial mass and substantially elevated long-chain fatty acid uptake capacity. Moreover, uptake of lipids from autologous control and MM BM plasma suppressed $CD8^+$ T-cell mitochondrial mass and cytokine expression, which were significantly higher in cells cultured in PB plasma or lipid-depleted BM plasma. These findings agree with accumulating studies indicating that lipid uptake from tumor microenvironments impairs immune cell mitochondrial and effector function.[19,20,23,32] Furthermore, these data imply that this immune-regulatory mechanism occurs even in the healthy BM niche but that it may compound disease-driven T-cell metabolic changes. Notably, $CD4^+$ T cells within patient samples demonstrated lower lipid uptake and were also unaffected by BM lipids in vitro, despite being suppressed by BM plasma, indicating that lipid-mediated suppression is restricted to $CD8^+$ T cells and alternate mechanisms regulate BM $CD4^+$ T-cell activity.

Assessment of single-cell transcriptomic data from patients with MM identified BM $CD8^+$ T-cell expression of the long-chain fatty acid transporters FATP1 and FATP5. Moreover, FATP1 blockade restored T-cell function in BM plasma, indicating that it could be

Figure 2 (continued) and PB $CD8^+$ and $CD4^+$ T cells directly compared for all patients combined. (J) C_{16}-BODIPY uptake of panel J NV, CM, EM, and EMRA BM $CD8^+$ T-cell subsets and subsets expressing TIGIT and/or PD-1 as indicated from samples with MM at diagnosis (n = 12). (K) Lipid peroxidation capacity of $CD8^+$ T cells within BM and PB mononuclear cells from patients with MM at diagnosis (n = 4), assessed using the lipid peroxidation probe Bodipy 581/591. For panels A-B,G,I-J, significance was calculated using 1-way ANOVA or for panels C-D (bars) and E,H (bars) 2-way ANOVA and Sidak multiple comparison tests; for panels C-D,H (circles) and K, a paired *t* test was used; and for panel F, Pearson correlation; $^*P < .05$, $^{**}P < .01$, $^{***}P < .0001$, and $^{****}P < .00001$.

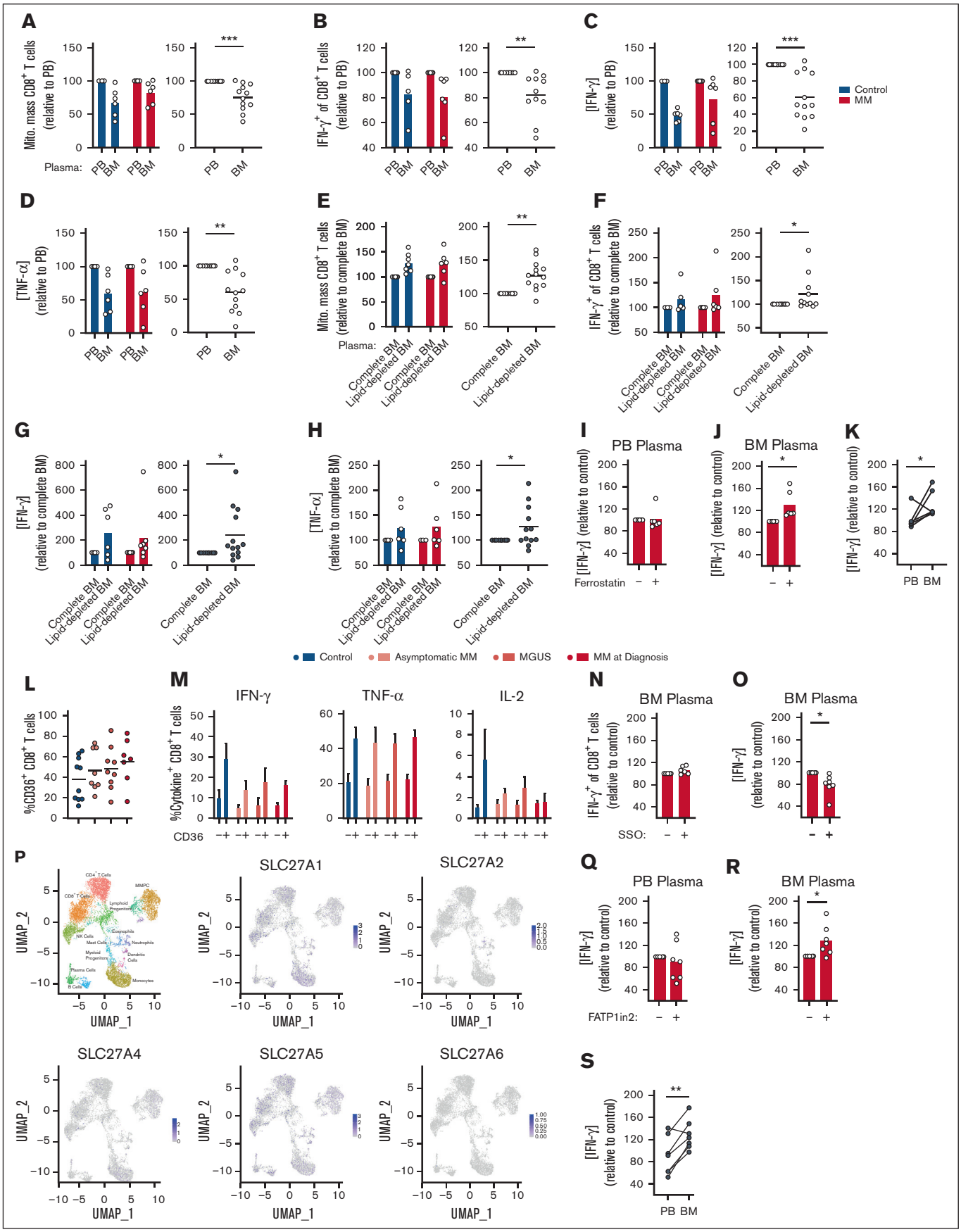

Figure 3.

targeted to augment function of endogenous or therapeutic T cells in the MM BM. Notably, FATP1 blockade had little effect on T cells cultured in PB plasma, suggesting that it targets an immunosuppressive axis unique to the BM microenvironment. Indeed, FATP1 substrates are enriched in the BM, an environment abundant in adipocytes[26] in which local lipolysis is induced by malignant MMPCs.[29] FATP1 transports fatty acids with chain lengths between 12 and 24 carbons.[40-42] Several studies report altered lipid abundance in PB plasma in MM, including enrichment of palmitate (C16) and long-chain acyl-carnitine species (C14-18) compared with in healthy controls.[43-45] Of note, palmitate exposure inhibits protective functions of NK cells and $CD8^+$ T cells[19,20] whereas acyl-carnitines induce TReg apoptosis via caspase activation,[46] highlighting the potential of these lipid species to modulate immune cell function. To date, 1 study has assessed BM plasma lipid profiles in MM, which compared these with MGUS samples rather than controls. Here, increased abundance of complex lipids including phosphatidylethanolamines, lactosylceramides, and phosphatidylinositols was observed in MGUS, whereas total free fatty acid profiles were similar.[47] MMPCs also use FATP1, alongside FATP4, to acquire adipocyte-derived long-chain fatty acids, which are oxidized to support growth and treatment resistance.[28,48] Furthermore, inhibition of fatty acid binding proteins inhibits MMPC growth and survival.[49] Therefore, a lipid-uptake–targeting strategy could impair malignant cell growth and augment antitumor immunity in MM, acting specifically within the BM microenvironmental niche. Further support for an approach to modulate T-cell lipid uptake in MM is provided here by analysis of samples from patients in relapse vs those in remission. Strikingly, although T cells in these samples were very similar in terms of abundance, phenotype, and immune-checkpoint expression, the significantly improved function of T cells from patients in remission was accompanied by restored mitochondrial mass and decreased lipid uptake. Taken together, these data identify that $CD8^+$ T-cell functionality is decreased within the BM environment, particularly at onset of MM. This is associated with significantly increased uptake of long-chain fatty acids, of which prevention improves $CD8^+$ T-cell activity. Therefore, strategies to block or limit lipid uptake may augment T-cell function in MM and improve efficacy of T-cell–directed immunotherapies in this disease.

Acknowledgments

The authors gratefully acknowledge the contribution to this study made by the University of Birmingham's Human Biomaterials Resource Centre, which was set up through the Birmingham Science City, Experimental Medicine Network of Excellence Project.

This work was funded by Leukaemia UK John Goldman Fellowship and Blood Cancer UK Project grant 21007 (S.D.), which also supported N.G. and H.M. T.F.-W. was supported by a Cancer Research UK PhD Studentship. C.E.-G. and D.A.T. are supported by Cancer Research UK Programme grant C42109/A24757. H.G. is supported by a British Society of Haematology Early-Stage Research grant. A.P.C. is a recipient of a Medical Research Council Career Development Fellowship (MR/V010182/1).

Authorship

Contribution: N.G. designed and performed research; H.G., E.L.B., T.F.-W., C.E.-G., H.M., F.K., D.J., and A.M. collected data and performed research; A.J.-B., K.F., and A.P.C. analyzed and interpreted data; D.A.T., S.B., and G.P. designed research; and S.D. designed and performed research, analyzed and interpreted data, performed statistical analysis, and wrote the manuscript.

Conflict-of-interest disclosure: A.P.C. is cofounder of Caeruleus Genomics Ltd and is an inventor on several patents related to sequencing technologies filed by Oxford University Innovations. D.A.T. undertakes paid consultancy work for Sitryx Ltd. H.G. completed a PhD funded by The Binding Site Ltd. The remaining authors declare no competing financial interests.

ORCID profiles: N.G., 0000-0002-0396-5241; A.J.-B., 0000-0001-9658-5354; K.F., 0000-0002-0330-8305; D.A.T., 0000-0003-0499-2732; S.D., 0000-0002-4598-6518.

Correspondence: Sarah Dimeloe, Institute of Biomedical Research, Institute of Immunology and Immunotherapy, College of Medical and Dental Sciences, Room 432, University of Birmingham, Edgbaston, Birmingham B15 2TT, United Kingdom; email: s.k.dimeloe@bham.ac.uk.

Figure 3. $CD8^+$ T-cell function is impaired by BM long-chain fatty acid uptake via FATP1. (A-D) BM mononuclear cells from controls (n = 6) or patients with MM who had relapsed (n = 6) were cultured in autologous PB or BM plasma as indicated for 72 hours with stimulation via CD3/CD28. (A) $CD8^+$ T-cell mitochondrial mass was assessed by flow cytometry using MVG and is shown for each group (left) and both groups combined (right). (B) At 72 hours, T cells were activated with PMA/ionomycin and expression of IFN-γ was assessed within $CD8^+$ T cells by flow cytometry. (C-D) IFN-γ and TNF-α in cell culture supernatants was measured by ELISA. (E-H) BM mononuclear cells were cultured and assessed as in panels A-D but in either complete or lipid-depleted BM autologous plasma as indicated. (I-K) BM mononuclear cells from patients with MM at diagnosis (n = 6) were cultured in autologous PB (I,K) or BM (J-K) plasma as in panels A-D, in absence or presence of ferrostatin and assessed for IFN-γ expression by ELISA. (L) Proportion of $CD8^+$ T cells expressing CD36 within indicated BM mononuclear cell samples from controls (n = 10), individuals with MGUS (n = 8), asymptomatic MM (asymptomatic; n = 9), or MM at diagnosis (diagnosis; n = 7) were assessed by flow cytometry. (M) Expression of IFN-γ, TNF-α, and IL-2 by $CD36^+$ or $CD36^-$ $CD8^+$ T cells within indicated BM mononuclear cell samples as in panel L. (N-O) BM mononuclear cells from patients with MM at diagnosis (n = 7) were cultured in autologous BM plasma as in panel A-D, in absence or presence of the CD36 inhibitor, SSO, and assessed for IFN-γ expression within $CD8^+$ T cells by flow cytometry (N) or by ELISA (O). (P) single-cell RNA-sequencing UMAP projections of BM mononuclear cells from 2 patients with newly diagnosed MM, with cell type annotation (top left) and transcript abundance of indicated genes overlaid. (Q-S) BM mononuclear cells from patients with MM at diagnosis (n = 7) were cultured in autologous PB (Q,S) or BM (R-S) plasma as in panels A-D, in absence or presence of the FATP1 inhibitor, FATP1in2, and assessed for IFN-γ expression by ELISA. Significance was calculated using Wilcoxon matched-pairs signed rank test for panels A-H (circles), I-J,N-O,Q-R; and paired *t* test for panels K,S; $*P < .05$, $**P < .01$, and $***P < .0001$. UMAP, Uniform Manifold Approximation and Projection.

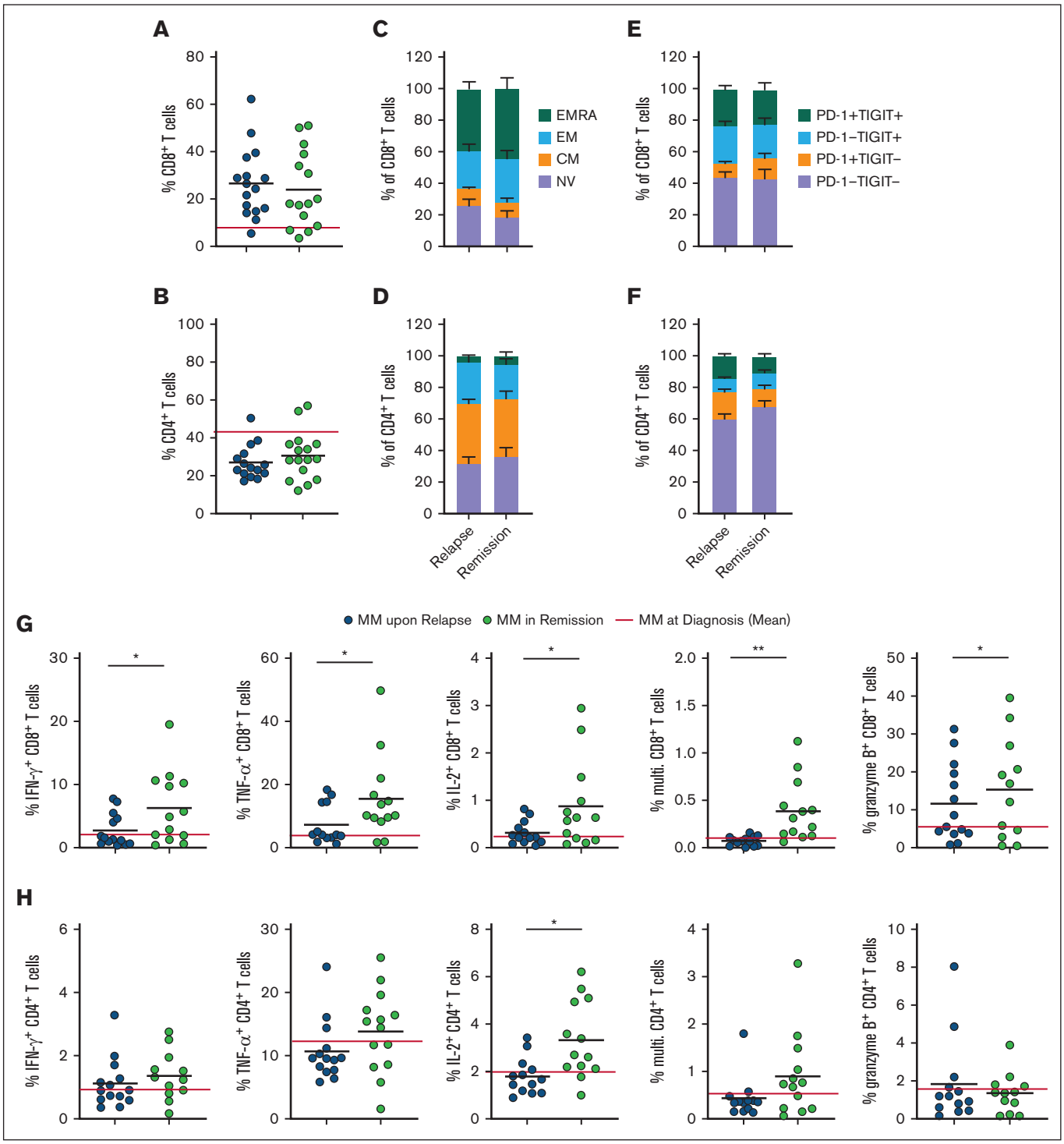

Figure 4. Functional and metabolic features of CD8$^+$ T cells are restored in patients with MM in remission but not in patients with relapsed MM. (A-B) Proportion of (A) CD8$^+$ and (B) CD4$^+$ T cells within BM mononuclear cells from patients with relapsed MM (n = 12) and patients with MM in remission (n = 12), the red line indicates controls (n = 10). (C-D) Proportions of NV, CM, EM, and EMRA (C) CD8$^+$ and (D) CD4$^+$ T cells in indicated BM samples. (E-F) Percentage of PD-1$^-$TIGIT$^-$, PD-1$^+$TIGIT$^-$, PD-1$^-$TIGIT$^+$, and PD-1$^+$TIGIT$^+$ (E) CD8$^+$ and (F) CD4$^+$ T cells in BM mononuclear cells from indicated samples. (G-H) Proportion of (G) CD8$^+$ and (H) CD4$^+$ T cells within BM mononuclear cells from each group expressing IFN-γ, TNF-α, IL-2, all 3 of these cytokines (multifunctional), or granzyme B after 4 hours of stimulation via CD3/CD28 Brefeldin A. (I) Correlation of percentage of malignant plasma cells within the BM sample with frequency of cells positive (+) for the indicated cytokines for samples combined for patients with MM at diagnosis (n = 12), patients with relapsed MM (n = 14), and patients with MM in remission (n = 12). (J) C_{16}-BODIPY uptake and (K) mitochondrial mass of BM and PB CD8$^+$ T cells within each group as indicated. The red line indicates the mean value in patients with MM at diagnosis. For panels A-B,G-H,J-K (circles), significance was calculated using unpaired *t* test; for panel I, Pearson correlation; and 2-way ANOVA and Sidak multiple comparison tests for panel J; *$P < .05$ and **$P < .01$.

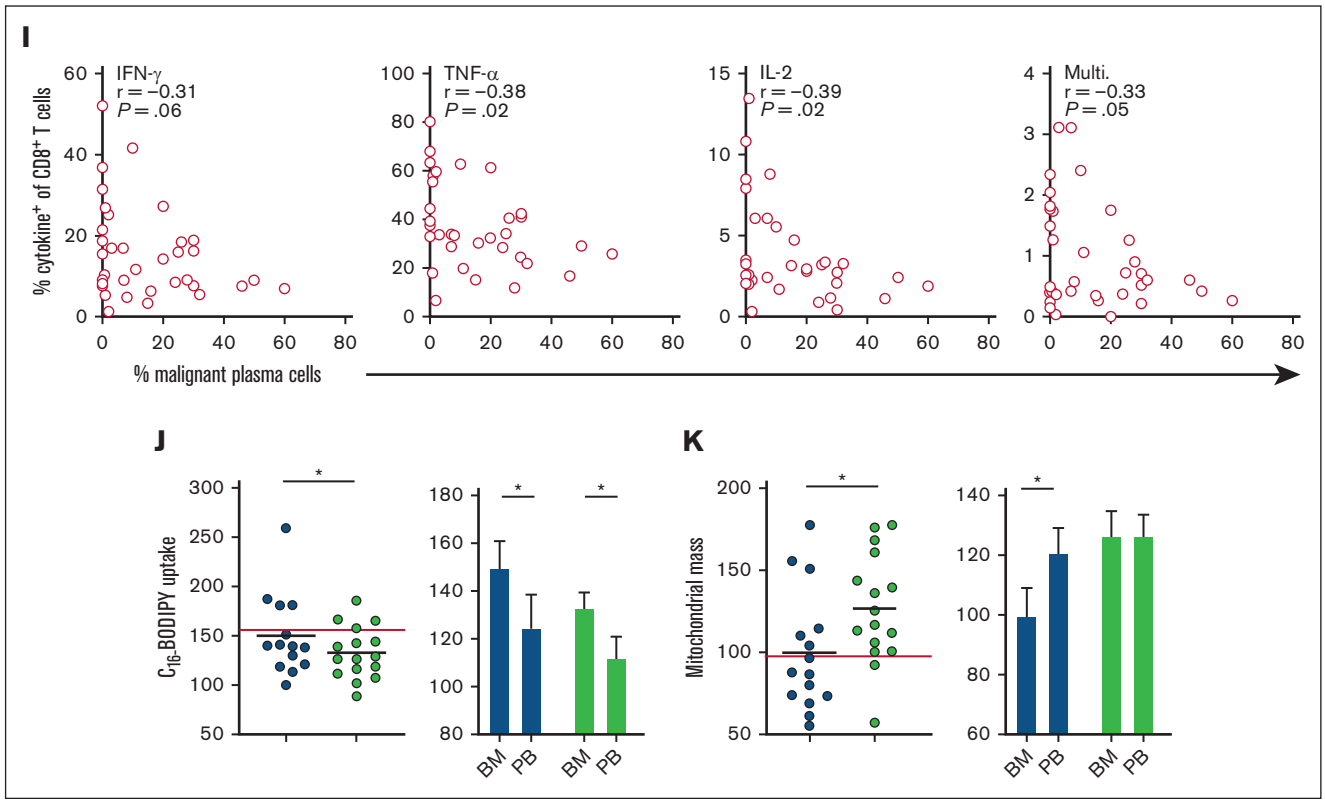

Figure 4 (continued)

References

1. Dhodapkar MV, Krasovsky J, Osman K, Geller MD. Vigorous premalignancy-specific effector T cell response in the bone marrow of patients with monoclonal gammopathy. *J Exp Med*. 2003;198(11):1753-1757.
2. Fichtner S, Hose D, Engelhardt M, et al. Association of antigen-specific T-cell responses with antigen expression and immunoparalysis in multiple myeloma. *Clin Cancer Res*. 2015;21(7):1712-1721.
3. Zelle-Rieser C, Thangavadivel S, Biedermann R, et al. T cells in multiple myeloma display features of exhaustion and senescence at the tumor site. *J Hematol Oncol*. 2016;9(1):116.
4. Goodyear OC, Essex S, Seetharam A, Basu S, Moss P, Pratt G. Neoplastic plasma cells generate an inflammatory environment within bone marrow and markedly alter the distribution of T cells between lymphoid compartments. *Oncotarget*. 2017;8(18):30383-30394.
5. Wang JN, Cao XX, Zhao AL, Cai H, Wang X, Li J. Increased activated regulatory T cell subsets and aging Treg-like cells in multiple myeloma and monoclonal gammopathy of undetermined significance: a case control study. *Cancer Cell Int*. 2018;18:187.
6. Kourelis TV, Villasboas JC, Jessen E, et al. Mass cytometry dissects T cell heterogeneity in the immune tumor microenvironment of common dysproteinemias at diagnosis and after first line therapies. *Blood Cancer J*. 2019;9(9):72.
7. Alrasheed N, Lee L, Ghorani E, et al. Marrow-infiltrating regulatory T cells correlate with the presence of dysfunctional CD4(+)PD-1(+) cells and inferior survival in patients with newly diagnosed multiple myeloma. *Clin Cancer Res*. 2020;26(13):3443-3454.
8. Vuckovic S, Bryant CE, Lau KHA, et al. Inverse relationship between oligoclonal expanded CD69- TTE and CD69+ TTE cells in bone marrow of multiple myeloma patients. *Blood Adv*. 2020;4(19):4593-4604.
9. Bailur JK, McCachren SS, Doxie DB, et al. Early alterations in stem-like/resident T cells, innate and myeloid cells in the bone marrow in preneoplastic gammopathy. *JCI Insight*. 2019;5(11):e127807.
10. Lesokhin AM, Ansell SM, Armand P, et al. Nivolumab in patients with relapsed or refractory hematologic malignancy: preliminary results of a phase Ib study. *J Clin Orthod*. 2016;34(23):2698-2704.
11. Zanwar S, Nandakumar B, Kumar S. Immune-based therapies in the management of multiple myeloma. *Blood Cancer J*. 2020;10(8):84.
12. Marchingo JM, Cantrell DA. Protein synthesis, degradation, and energy metabolism in T cell immunity. *Cell Mol Immunol*. 2022;19(3):303-315.
13. Chapman NM, Chi H. Metabolic adaptation of lymphocytes in immunity and disease. *Immunity*. 2022;55(1):14-30.

14. Ho PC, Bihuniak JD, Macintyre AN, et al. Phosphoenolpyruvate is a metabolic checkpoint of anti-tumor T cell responses. *Cell*. 2015;162(6):1217-1228.
15. Chang CH, Qiu J, O'Sullivan D, et al. Metabolic competition in the tumor microenvironment is a driver of cancer progression. *Cell*. 2015;162(6):1229-1241.
16. Reinfeld BI, Madden MZ, Wolf MM, et al. Cell-programmed nutrient partitioning in the tumour microenvironment. *Nature*. 2021;593(7858):282-288.
17. Scharping NE, Menk AV, Moreci RS, et al. The tumor microenvironment represses T cell mitochondrial biogenesis to drive intratumoral T cell metabolic insufficiency and dysfunction. *Immunity*. 2016;45(3):701-703.
18. Scharping NE, Rivadeneira DB, Menk AV, et al. Mitochondrial stress induced by continuous stimulation under hypoxia rapidly drives T cell exhaustion. *Nat Immunol*. 2021;22(2):205-215.
19. Michelet X, Dyck L, Hogan A, et al. Metabolic reprogramming of natural killer cells in obesity limits antitumor responses. *Nat Immunol*. 2018;19(12):1330-1340.
20. Manzo T, Prentice BM, Anderson KG, et al. Accumulation of long-chain fatty acids in the tumor microenvironment drives dysfunction in intrapancreatic CD8+ T cells. *J Exp Med*. 2020;217(8):e20191920.
21. Zhang C, Yue C, Herrmann A, et al. STAT3 activation-induced fatty acid oxidation in CD8+ T effector cells is critical for obesity-promoted breast tumor growth. *Cell Metab*. 2020;31(1):148-161.e5.
22. Liu X, Hartman CL, Li L, et al. Reprogramming lipid metabolism prevents effector T cell senescence and enhances tumor immunotherapy. *Sci Transl Med*. 2021;13(587):eaaz6314.
23. Xu S, Chaudhary O, Rodríguez-Morales P, et al. Uptake of oxidized lipids by the scavenger receptor CD36 promotes lipid peroxidation and dysfunction in CD8+ T cells in tumors. *Immunity*. 2021;54(7):1561-1577.e7.
24. Dyck L, Prendeville H, Raverdeau M, et al. Suppressive effects of the obese tumor microenvironment on CD8 T cell infiltration and effector function. *J Exp Med*. 2022;219(3):e20210042.
25. Prendeville H, Lynch L. Diet, lipids, and antitumor immunity. *Cell Mol Immunol*. 2022;19(3):432-444.
26. Morris EV, Edwards CM. Bone marrow adiposity and multiple myeloma. *Bone*. 2019;118:42-46.
27. Marinac CR, Birmann BM, Lee IM, et al. Body mass index throughout adulthood, physical activity, and risk of multiple myeloma: a prospective analysis in three large cohorts. *Br J Cancer*. 2018;118(7):1013-1019.
28. Trotter TN, Gibson JT, Sherpa TL, Gowda PS, Peker D, Yang Y. Adipocyte-lineage cells support growth and dissemination of multiple myeloma in bone. *Am J Pathol*. 2016;186(11):3054-3063.
29. Panaroni C, Fulzele K, Mori T, et al. Multiple myeloma cells induce lipolysis in adipocytes and uptake fatty acids through fatty acid transporter proteins. *Blood*. 2022;139(6):876-888.
30. Chang CH, Curtis JD, Maggi LB, et al. Posttranscriptional control of T cell effector function by aerobic glycolysis. *Cell*. 2013;153(6):1239-1251.
31. Gubser PM, Bantug GR, Razik L, et al. Rapid effector function of memory CD8+ T cells requires an immediate-early glycolytic switch. *Nat Immunol*. 2013;14(10):1064-1072.
32. Ma X, Xiao L, Liu L, et al. CD36-mediated ferroptosis dampens intratumoral CD8+ T cell effector function and impairs their antitumor ability. *Cell Metab*. 2021;33(5):1001-1012.e5.
33. Kurata K, James-Bott A, Tye MA, et al. Prolyl-tRNA synthetase as a novel therapeutic target in multiple myeloma. *Blood Cancer J*. 2023;13(1):12-12.
34. Granja JM, Klemm S, McGinnis LM, et al. Single-cell multiomic analysis identifies regulatory programs in mixed-phenotype acute leukemia. *Nat Biotechnol*. 2019;37(12):1458-1465.
35. Anderson CM, Stahl A. SLC27 fatty acid transport proteins. *Mol Aspects Med*. 2013;34(2-3):516-528.
36. Kwon M, Kim CG, Lee H, et al. PD-1 blockade reinvigorates bone marrow CD8+ T cells from patients with multiple myeloma in the presence of TGFβ inhibitors. *Clin Cancer Res*. 2020;26(7):1644-1655.
37. Spencer JA, Ferraro F, Roussakis E, et al. Direct measurement of local oxygen concentration in the bone marrow of live animals. *Nature*. 2014;508(7495):269-273.
38. Sinclair LV, Barthelemy C, Cantrell DA. Single cell glucose uptake assays: a cautionary tale. *Immunometabolism*. 2020;2(4):e200029.
39. Manier S, Ingegnere T, Escure G, et al. Current state and next-generation CAR-T cells in multiple myeloma. *Blood Rev*. 2022;54:100929.
40. DiRusso CC, Li H, Darwis D, Watkins PA, Berger J, Black PN. Comparative biochemical studies of the murine fatty acid transport proteins (FATP) expressed in yeast. *J Biol Chem*. 2005;280(17):16829-16837.
41. Huang J, Zhu R, Shi D. The role of FATP1 in lipid accumulation: a review. *Mol Cell Biochem*. 2021;476(4):1897-1903.
42. Hall AM, Wiczer BM, Herrmann T, Stremmel W, Bernlohr DA. Enzymatic properties of purified murine fatty acid transport protein 4 and analysis of acyl-CoA synthetase activities in tissues from FATP4 null mice. *J Biol Chem*. 2005;280(12):11948-11954.
43. Jurczyszyn A, Czepiel J, Gdula-Argasińska J, et al. Plasma fatty acid profile in multiple myeloma patients. *Leuk Res*. 2015;39(4):400-405.
44. Lodi A, Tiziani S, Khanim FL, et al. Proton NMR-based metabolite analyses of archived serial paired serum and urine samples from myeloma patients at different stages of disease activity identifies acetylcarnitine as a novel marker of active disease. *PLoS One*. 2013;8(2):e56422.
45. Steiner N, Müller U, Hajek R, et al. The metabolomic plasma profile of myeloma patients is considerably different from healthy subjects and reveals potential new therapeutic targets. *PLoS One*. 2018;13(8):e0202045.

46. Hulme HE, Meikle LM, Wessel H, et al. Mass spectrometry imaging identifies palmitoylcarnitine as an immunological mediator during Salmonella typhimurium infection. *Sci Rep*. 2017;7(1):2786.

47. Gonsalves WI, Broniowska K, Jessen E, et al. Metabolomic and lipidomic profiling of bone marrow plasma differentiates patients with monoclonal gammopathy of undetermined significance from multiple myeloma. *Sci Rep*. 2020;10(1):10250.

48. Tirado-Velez JM, Joumady I, Saez-Benito A, Cozar-Castellano I, Perdomo G. Inhibition of fatty acid metabolism reduces human myeloma cells proliferation. *PLoS One*. 2012;7(9):e46484.

49. Farrell M, Fairfield H, Karam M, et al. Targeting the fatty acid binding proteins disrupts multiple myeloma cell cycle progression and MYC signalin. *Elife*. 2023;12:e81184.